Biointerface Research in Applied Chemistry
Open-Access Journal (ISSN: 2069-5837)

Article
Volume 13, Issue 6, 2023, 568
https://doi.org/10.33263/BRIAC136.568

Benzyl Isothiocyanate (BITC) Instigated Selective Cytotoxicity Effects on Breast Cancer Cell Line, MCF-7 Cells and Human Normal Fibroblast Cells, CRL-2522 and its Bioavailability in Miswak (*Salvadora persica* L.): *In vitro* and *In silico* Perspective

N. H. A. Kadir [1,*], M. H. A. Rahaman [2], M. Shahinuzzaman [3,*], Zahira Yaakob [4], Mahboob Alam [5,*]

[1] BIOSES RIG, Faculty of Science and Marine Environment, Universiti Malaysia Terengganu, 21030 Kuala Nerus, Terengganu, Malaysia
[2] Solution Biologic Sdn Bhd, Technology Park Malaysia, 57000 Kuala Lumpur, Wilayah Persekutuan, Malaysia
[3] Institute of Fuel Research and Development, Bangladesh Council of Scientific and Industrial Research (BCSIR), Dhaka 1205, Bangladesh
[4] Department of Chemical and Process Engineering, Universiti Kebangsaan Malaysia, UKM Bangi 43600, Selangor, Malaysia
[5] Division of Chemistry and Biotechnology, Dongguk University, 123 Dongdae-ro, Gyeongju, Republic of Korea
* Correspondence: nurulhuda@umt.edu.my (N.H.A.K.), shahinchmiu@gmail.com (M.S.), mahboobchem@gmail.com (M.A.);

Scopus Author ID 57226661617
Received: 7.12.2022; Accepted: 10.01.2023; Published: 19.03.2023

Abstract: Benzyl isothiocyanate (BITC) is one of the natural products that has been identified as a potent anticancer agent. BITCs are the degradation products of glucosinolates resulting from hydrolysis in plants such as Brassica vegetables. In this study, cytotoxicity effects, MTT assay, determination of reactive oxygen species (ROS), Caspase 3/7 level, AO/EtBr for apoptosis assay, and Western blotting after exposure to BITC were investigated. Molecular docking of BITC with human 5.10-methyltetrahydrofolate synthetase receptor, MTHFS (PDB:3HY3), and epidermal growth factor receptor tyrosine kinase (EGFRK) domain (PDB:1M17) were used to explore protein-ligand interactions. The results showed that BITC exhibited a cytotoxicity effect on MCF-7 cancer cells with an EC50 value of 23.4 µM. Interestingly, BITC slightly induced cytotoxicity effect towards normal human fibroblast cells. The treated MCF-7 cell lines with BITC showed the regulation of NRF-2, p38, glutathione-S-transferase (GST), BCL-2, p-ERK, and ERK 1/2 protein expression, as well as NF-κB and MAPK gene expression. Additionally, 6.25% BITC content was obtained from the methanol-hexane extraction of Miswak. The current study may shed light on the significance of BITC as a potent inhibitor of cancer cells. Furthermore, the *in silico* study provides a protein and ligand interaction profile for a better understanding of the mechanical approach to the cytotoxicity effect of BITC by triggering MAPK proteins.

Keywords: cell death; oxidative stress; MCF-7; glucosinolates; benzyl isothiocyanate; molecular docking.

1. Introduction

Cruciferous vegetables such as radish, cabbage, cauliflower, broccoli, mustard, and horseradish are potential dietary components that may reduce cancer risk [1]. Currently, the

use of dietary bioactive compounds is becoming an alternative to control and treat cancer. For example, isothiocyanates (ITCs) present in cruciferous vegetables, *Carica papaya* [2,3], *Moringa oleifera* [4], and *Salvadora persica* [5,6], have potential chemoprevention activity against several human malignancies including pancreatic cancer and breast cancer [7,8]. Besides, glucosinolates are chemoprevention's most studied bioactive components [1,7]. Glucosinolates can be converted to benzyl isothiocyanate (BITC) through the hydrolysis of myrosinase enzyme, which has been reported to possess anticancer activity [9].

Based on numerous studies, BITC was claimed to be a natural chemoprevention, antitumor and cytotoxic agent [10-15]. BITC also possesses other therapeutic effects such as anti-inflammatory [16] and antimicrobial [17-19]. Epidemiological studies have also indicated that increased consumption of vegetables containing ITCs reduces cancer incidence at several sites [20,21]. Although numerous research has shown the cytotoxicity effect of BITC on various cancer cell lines, limited studies conducted molecular *in vitro* and *in silico* approaches on the mechanism of cytotoxic effects of BITC in cancer cells were reported.

This study aims to evaluate the cytotoxicity effect of BITC on MCF-7 cancer cells and the human fibroblast cell, CRL-2522, to compare the effect of them. This has been conducted to evaluate the regulation of oxidative stress and MAPK (Mitogen-activated Protein Kinase) pathway to induce cell death in MCF-7 cell lines after exposure to BITC [22,23]. This study also used molecular docking, which has emerged as a useful tool for drug discovery due to the effectiveness and usefulness of recent advances in the field of *in silico* methods and bioinformatics for characterizing molecular interactions. Molecular docking techniques can be utilized to understand and visualize drug-protein interactions at the atomic level, helping us to understand better and explain the activity of molecules in target protein binding sites. Finally, we quantified the BITC present in the Miswak extract using Gas- Chromatography/Mass Spectroscopy analysis. Extraction technique using two solvents (methanol and water) for extraction was performed to evaluate which solvents are the best solvent for BITC extraction. BITC derives from the hydrolysis of benzylglucosinolates by myrosinase; water is a vital solvent in the development of BITC. Methanol is a polar solvent consisting of a small percentage of water and may help extract glucosinolate and its hydrolysis products [1], and it was used to extract BITC in the study.

2. Materials and Methods

2.1. Chemicals.

BITC and phosphate buffer saline were purchased from Sigma-Aldrich, USA. RPMI 1640 (Gibco), fetal bovine serum (Gibco), trypsin-EDTA (0.25%) (Gibco), and penicillin-streptomycin (Gibco) were purchased from Thermo Fisher Scientific (Waltham, MA USA). MTT (3-(4,5-Dimethylthiazol-2-yl)-2,5-diphenyltetrazolium bromide) reagent was purchased from Invitrogen (Paisley, Scotland, UK). DCM (Dichloromethane), Methanol, and Hexane were purchased from Sigma Aldrich, USA. All other chemicals, unless stated in the text, were purchased from Sigma Aldrich, USA.

2.2.Cell culture.

MCF-7 and CRL-2522 cell lines purchased from the American Type Culture Collection (ATCC) were used in this study. MCF-7 cell lines were maintained in RPMI 1640 media, and CRL-2522 cells were cultured in a complete medium of Eagle's Minimum Essential Medium

(EMEM) (ATCC, USA). Both types of cells were supplemented with 10% fetal bovine serum and incubated in a 5% CO_2 incubator at 37°C.

2.3. MTT assay.

Cytotoxicity of BITC was determined using MTT (Invitrogen, Life Technologies). MCF-7 cell lines were harvested and seeded ($5x10^3$ cells/well) in 96 well plates and left overnight in a humidified incubator with 5% CO_2 at 37°C to equilibrate. Ten µL of 0.1% DMSO as control BITC (concentrations of 1000, 100, 10, 1, and 0.1 µM) were added into 90 µL media containing MCF-7 cell lines and incubated for 24 and 48 hours. At the end of the incubation period, MTT reagent (50 µl, 50 mg/mL in PBS) was added to each well and incubated for 4 hours. The absorbance values were measured at the wavelength of 570 nm by using Varioskan™ Flash Multimode Reader (Thermo Fisher Scientific, USA).

2.4. Determination of reactive oxygen species (ROS).

ROS procedure was followed based on the study by Kadir *et al*. [17] with several modifications. $5x10^5$ MCF-7 cells were seeded in each well of 24 well plates and left overnight in a 37°C humidified incubator supplemented with 5% CO_2. 2,7-dichlorofluorescein diacetate (DCFDA) solution was prepared by diluting with DMSO. Fifty (50) mM DCFDA was added into each well and incubated for 30 minutes. All media in each well were discarded and washed 2 times with PBS. Four hundred and fifty (450) µL of new media was added into each well. The treated cells were immediately incubated at 37ºC at 5% CO_2. The fluorescence DCF intensity was measured fluorometrically at an excitation of 485 nm and an emission of 530 nm.

2.5. Caspase 3/7 level.

MCF-7 ($1x10^4$ cells/mL) cells were cultured in 96 well plates in controlled humidified conditions overnight (37ºC, 5% CO_2). Caspase 3/7 was measured after treatment using FAM-FLICA® Caspase Assay Kits, and the procedure was followed according to the manufacturer protocol (excitation: 488nm and emission: 530 nm) (Immunochemistry Technologies, USA).

2.6. AO/EtBr (Acridine orange and ethidium bromide) dual staining for apoptosis assay.

MCF-7 cells were seeded in six-well plates with $1×10^5$ cells/mL for each of the wells and were incubated at 37°C in a 5% CO_2 incubator overnight before treatment. AO and EtBr (Sigma Aldrich, USA) were dissolved separately in PBS with sterile conditions. Cells were incubated for 30 minutes with the final concentration of 2 µM AO and 6 µM EtBr in the culture system after 24 hours of treatment. Morphology of both the treated and untreated cells was observed and captured by inverted fluorescence microscopy (Olympus, Japan) with a DAPI-blue UV fluorescence filter. The images were captured using CellSens software.

2.7. Western blotting.

MCF-7 cell lines ($5 x 10^5$ cells) with 0.01% DMSO acted as a control, and the cells were treated with 30 µM BITC for 24 h and 48 h in 6 plates. The treated cells were dissociated and centrifuged (2000 rpm, 5 min, 4°C) to pellet the cells. Proteins from the treated cells' samples were extracted using NucleoSpin® RNA/Protein (Macherey-Nagel) protocol. Protein concentrations of the samples were obtained from Bradford assay, based on the protocol given

by Bio-Rad Protein Assay (Bio-Rad, USA). The extracted protein samples (20 µg) were separated using NuPAGE 4-12% bris-tris gels (Novex, Life Technologies, USA) according to the manufacturer protocol (Pub Part No. IM-8042) and transferred onto PVDF (Polyvinylidene Fluoride) membrane using a semi-dry transfer system (Bio-Rad, USA). PVDF membranes were incubated overnight with primary antibodies at 4 °C followed by incubation with HRP-conjugated secondary antibodies for an hour at room temperature. The following antibodies of p38 MAPK (D13E1), XP®Rabbit mAb (Cell Signaling) (with a ratio of 1:1000 dilution), GST (glutathione-S-Transferase) Tag Antibody (A-5800) (Thermo Fisher Scientific) (with a ratio of 1:600 dilution), Anti-NRF-2 (Nuclear factor erythroid 2-related factor 2) (AB89443, with a ratio of 1:1000 dilution, Abcam, USA), Bcl-2 (B-cell Lymphoma 2) (SC-7382, with a ratio of 1:1000 dilution, Santa Cruz), ERK1/2 (SC-514302, 1:1000 dilution, Santa Cruz), p-ERK (SC-7383, with a ratio of 1:1000 dilution, Santa Cruz) and anti-β-actin (AM4302, with a ratio of 1: 5,000 dilution, Ambion, USA) were used as primary antibodies to perform western blotting. Whereas HRP-conjugated Goat anti-Rabbit IgG (H+L) Secondary Antibody (G-21234, with a ratio of 1:2000 dilution) and HRP-conjugated anti-mouse secondary antibodies (A16072, with a ratio of 1:2,200 dilution) (Life Technologies, USA) were used as secondary antibodies. The image of targeted protein bands was normalized with the total protein content on the PVDF membrane and analyzed by using ImageLab software (Bio-Rad, USA).

2.8. Molecular docking.

The BITC was inserted into NMR structures of human 5,10-methenyltetrahydrofolate synthetase (MTHFS) (PDB:3HY3) and epidermal growth factor receptor tyrosine kinase (EGFRK) domain (PDB:1M17) and were carried out using AutoDock 4.2 program for molecular docking analysis. MTHFS helps cell growth and proliferation by supplying them with vital components. MTHFS inhibition has been shown to suppress the development of human MCF-7 breast cancer cells [18]. EGFR kinase, on the other hand, has a physiological function in regulating epithelial tissue growth and homeostasis. In pathological environments, EGFR is a tumorigenesis catalyst, specifically in lung cancer, breast cancer, and even glioblastoma [19]. Both receptors (PDB:3HY3 and 1M17) and BITC were retrieved from the Protein Data Bank (PDB) and PubChem databases. The involvement of amino acids in active sites in the receptors was identified on the basis of the co-crystalline ligands attached to them. Prior to docking, 3D receptor and ligand (BITC) structures were subjected to protein and ligand preparations which included adding polar hydrogen, merging non-polar hydrogens, assigning Kollman charges for the receptors, adding Gasteiger charges for the ligand, including setting up rotatable bonds and saving into PDBQT format for further steps of docking. The receptors grid maps were designed to include not only active sites but also considerable portions of the surrounding surface, using the AutoGrid included in the AutoDock package as grid parameters (X = 50 Å, Y = 50 Å, Z = 50 Å number of points, and grid-centered at X= 6.395Å, Y = 20.927Å, Z = -2.914 Å for MTHFS (PDB:3HY3) and X=60 Å, Y=60 Å, Z=60 Å and grid-centered at X=7.309 Å, Y=32.217Å Z=42.21 Å with a grid spacing of 0.375 Å for EGFRK) domain (PDB:1M17). The best-docked pose of the ligand to receptors was selected based on the free energy of binding with the highest number of populations (largest cluster), and the selected pose was used to visualize and interact the ligand with receptors to understand the mechanistic approach for inhibition action.

2.9. Extraction of BITC from Miswak.

Two extraction processes consisting of water and solvent extraction were carried out using the maceration extraction process described by Kadir *et al*. and EL-Hefny *et al*. [20] with some modifications. Twenty (100) gm of dry Miswak powder was extracted by the maceration extraction process using water as the solvent. The extraction process was done by soaking with water for one week and repeated three times, where every filtration was done after 2 days intervals and combined with the extract. After extraction, the extract was dried using a rotary evaporator. Then 5 ml dichloromethane (DCM) was added to the dry extract, and the lower DCM layer was transferred to glass tubes using a hypodermal syringe. The extraction process was repeated by adding 5 ml of DCM. The DCM extract was combined and dried over anhydrous $MgSO_4$ (≈3g). The extract was then transferred to a glass pipette containing a plug of absorbent cotton, and the samples were filtered and used for GC-MS analysis.

On the other hand, for solvent extraction, twenty (20) gm of dry Miswak powder was extracted by a maceration extraction process using methanol and n-hexane (1:1 v/v) as the solvent. The extraction process was repeated three times at 2 days intervals and combined with the extract. After extraction, the extract was dried using a rotary evaporator at 45 °C. Then 5 ml Dichloromethane (DCM) was added to the dry extract, and the lower DCM layer was transferred to glass tubes using a hypodermal syringe. The extraction process was repeated by adding 5 ml of DCM. The DCM extract was combined and dried over anhydrous $MgSO_4$ (≈3g). The extract was then transferred to a glass pipette containing a plug of absorbent cotton, and the samples were filtered and used for GC-MS analysis [21].

2.10. The GC-MS analysis of Miswak extract.

The gas chromatography-mass spectrometer (GC-MS) analysis of Miswak extract was performed on an Agilent 7890A gas chromatograph (GC) directly coupled to the mass spectrometer system (MS) using an Agilent 5975C inert MSD (Mass Selective Detector) with a triple-axis detector with an Agilent Technologies capillary DB-5MS UI column (30 m in length; 0.25 mm i.d.; 0.25 mm film thickness), ionization voltage 70eV; all (Agilent, Santa Clara, CA, USA). The carrier gas was He and was used at a 1 mL/min flow rate. The oven temperature program was as follows: 50°C for 5 min, then 6°C/min to 270°C for 5 min. Run Time was 35min, maximum post temperature 310°C, and equilibrium time 50s. The MSD Chemstation was used to find all peaks in the raw GC chromatogram. The NIST 11 database library was used to identify the compounds by GC- MS analysis. The number of constituents was expressed as the percentage of peak area normalization.

2.11. Quantification of BITC from Miswak extract.

For the quantification of BITC, the standard pure BITC compound was purchased from the local supplier. The calibration curve was generated using four different concentrations (12.5, 25, 50, and 100 µg/mL) of standard BITC. From the standard curve ($y = 1.0388x + 9.7517$; $R^2 = 0.9595$), BITC was quantified, and the results were expressed as µg/ml.

2.12. Statistical analysis.

GraphPad Prism 5.0 was used for all analyses. One-way and two-way analysis of variance followed by Dunnett and Bonferonni multiple comparisons were performed,

respectively, to determine significant differences between treatment groups and controls. The analysis was done according to means ± SEM, and *P<0.05, ** P<0.01, *** P<0.001 are significant differences compared to the control.

3. Results and Discussion

3.1. Effects of BITC on cell viability.

The cytotoxic effects of BITC (0-100 µM) on MCF-7 cells and human fibroblast cells were determined using an MTT assay. The results shown in Figure 1 indicate that BITC is cytotoxic toward MCF-7 cells in a time- and dose-dependent manner. After the exposure to 100 µM BITC at 48h, the viability of MCF-7 cancer cells was reduced by 100%. The important issue raised by this study is whether these cytotoxicity effects were specific to cancer cells, which would be a large opportunity for cancer therapeutics. We tended to this inquiry by evaluating the impact of these treatments on human fibroblast cells, CRL-2522 as a model of non-cancerous cells. The viability of CRL-2522 cells reduced by 37.25% after the exposure to 100 µM BITC at 24h compared to the control. Overall, the exposure of every treatment (0-100 µM) on CRL-2522 cells 24 and 48h does not reach the level of EC50, suggesting that all treatment is not significantly toxic toward this non-cancerous model.

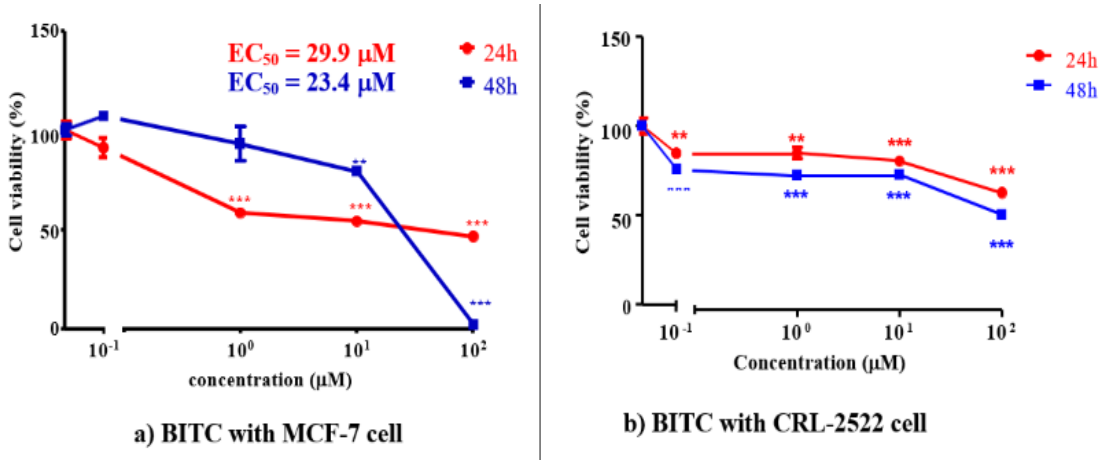

Figure 1. Cytotoxicity effect of treatment of MCF-7 cells and CRL-2522 cells with BITC at 24 and 48 h as assessed by MTT dye absorbance (570 nm). Cisplatin was chosen as a positive control. Results for MTT dye absorbance are shown as percentage cell viability. One-way ANOVA (Dunnett post-test) analysis was performed for each data set of means ± SEM for independent cultures (n=4), and *P<0.05, ** P<0.01, *** P<0.001 are significant differences compared to control.

This result is supported by the findings of Rahaman *et al*. [4,24], who stated that BITC treatment would trigger the MAPK pathway and lead to apoptosis during 24 h. Bitc exhibits anticancer potential by interfering with the signal transduction cascade that promotes cancer cell proliferation and progression. In addition, BITC possessed chemopreventative and therapeutic properties, which could be a novel approach to target prooncogenic pathways [25], which was investigated previously with different human cancer cells like cisplatin-resistant oral cancer CAR cells, NCI-H460 human lung cancer cells, and breast cancer cell [4,26] But in most cases, their fewer data about the effect of chemo-preventive agents on normal human cells. In addition, most chemo-preventive agents have a toxic effect on cancer cells and normal human fibroblast cells. Thus, evaluating the cytotoxicity effect of relative chemo-preventive agents on normal human fibroblast cells is also important.

3.2. Effect of reactive oxygen species (ROS).

H2DCFDA was used as a fluorescence probe to quantify ROS levels to evaluate the effects of BITC on intracellular redox changes. H2DCFDA will turn into fluorescent dichlorofluorescein (DCF) after getting oxidized by cellular ROS. Hydrogen peroxide as a positive control gave a high fluorescence DCF intensity, indicating a clear ROS response compared to the vehicle-treated control (0.05% DMSO exposure).

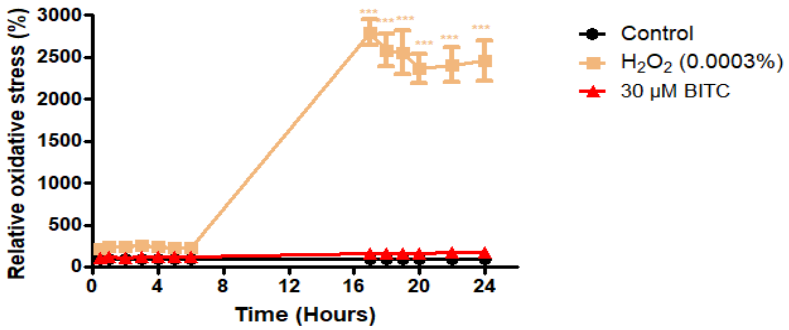

Figure 2. Reactive oxygen species (ROS) percentage level of MCF-7 cells with BITC and quercetin (30 µM) at 30 min, 1h, 2h, 3h, 4h, 5h, 6h, 17h, 18h, 19h, 20h, 22h, and 24h as assessed by DCFDA dye fluorometrically at excitation of 485 nm and emission of 530 nm. Each value is the mean ± SEM (n=3). Two-way ANOVA (Bonferroni post-test) analysis was performed, where *P<0.05, **P<0.01, ***P<0.001 are significant differences compared to the control.

The exposure of BITC (as shown in Figure 2) has caused a slight increase in ROS level until 24 h. ROS initiates the apoptotic cascade by oxidation of ASK (Apoptosis Signal-regulating Kinase) and activation of p38 MAPK and JNK (Jun N- terminal kinase) [27]. High levels of ROS also caused p53 accumulation and apoptosis [28-29]. However, the BITC

3.3. Expression analysis of various proteins and genes.

The treated MCF-7 cells were analyzed for p38, NRF-2, GST, ERK1/2. P-ERK and BCL-2 expression by western blot (Figure 3). Loading controls were labeled with the housekeeping protein β-actin, and the protein bands were normalized by stained-blotted protein on the PVDF membrane (Figure 3 b)). The intensity of protein band expression of treated MCF-7 cells with BITC differed compared to the control.

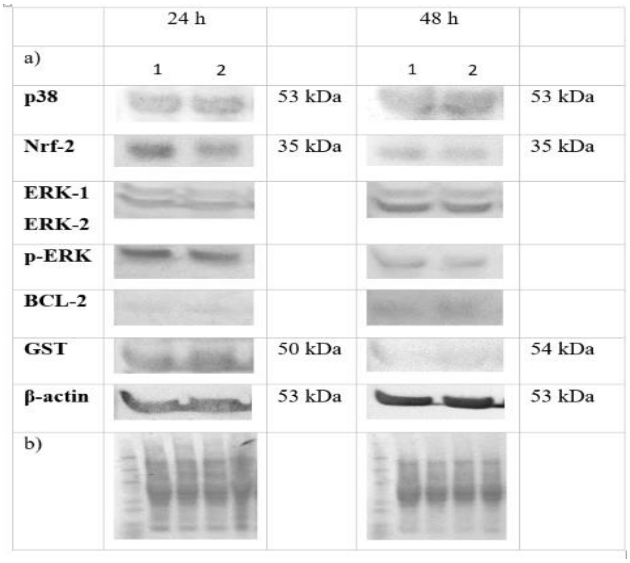

Figure 3. Expression analysis of MCF-7 cell protein after 24 and 48 h of the respective treatments (figure a); **(1)** control (0.01% DMSO); **(2)** 30 µM BITC respectively.

Figure 4 shows the percentage of relative band intensity of different protein expressions such as NRF-2, p38, GST, BCL-2, p-ERK, and ERK ½ for untreated and treated MCF-7 cells after 24 and 48 hours. The treatment of 30 µM BITC at 24 h increased the NRF- 2 expression significantly, but the expression of NRF-2 at 48h was not significant.

Treatment of BITC on MCF-7 cells significantly down-regulates the expression of ERK1/2 at 24. However, the ERK1/2 protein expression at 48 h was a non-significant difference compared to the control. Furthermore, phosphorylation of ERK (p-ERK) significantly increased after 24 h exposure to BITC to MCF-7 cells compared to the control. On the other hand, the p-ERK expression was not significant at 48 h. BITC significantly upregulated the expression of GST 1.83-fold higher than the control at 48 h. The expression of BCL-2 was significantly increased by the treatment of BITC at 24 h, but no significant difference at 48 h compared to the control. This suggests that BCL-2 expression was not persistent after 48 h of exposure, leading to cell death. NRF-2 protein expression was significantly upregulated at 24 h but not at 48 h, suggesting that MCF-7 cells exposed to BITC have lost their ability to regulate the antioxidant responses to overcome oxidants mediated by BITC.

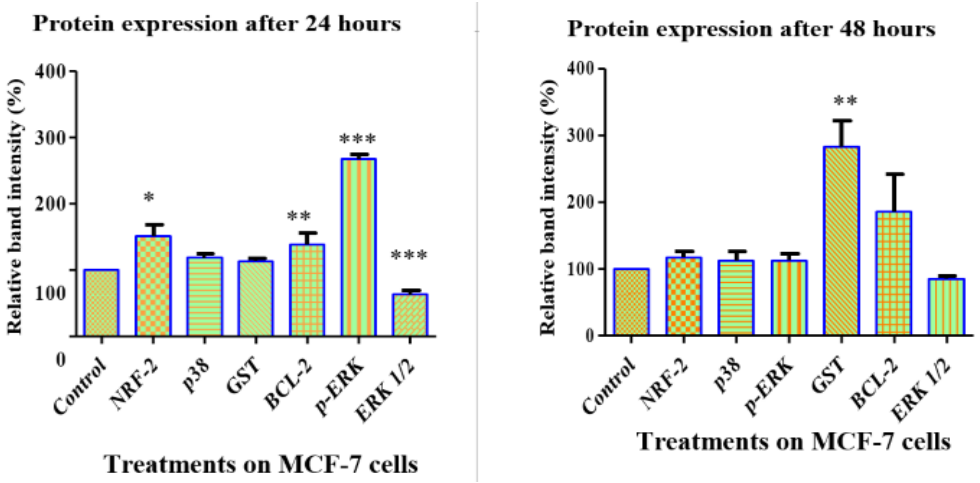

Figure 4. Percentage of relative band intensity of 6 different protein expressions for untreated and treated MCF-7 cells after 24 and 48 hours. The analysis was done by using Image Lab software version 5.2.1. Each value is the mean ± SEM (n=3). One-way ANOVA (Dunnett post-test) analysis was performed. *P<0.05, **P<0.01, ***P<0.001 are significant differences compared to control.

On the other hand, the treatment of 24 h of 30 µM BITC induced a marginal decrease of NF-κB and MAPK 3 (ERK1/2) gene expression treatment compared to the control (Figure 5). Activation of the MAP kinase pathway, specifically via JNK, triggered by many anticancer agents, leads to apoptosis [22,30,31]. BITC potentially inhibited cancer cell growth by inducing apoptosis by activating MAPK pathways. BITC caused cell cycle arrest at the G2/M phase and generated reactive oxygen species (ROS) [32-33]. This will promote oxidative stress causing cells to damage, and the MAPK pathway will activate in response to the damage.

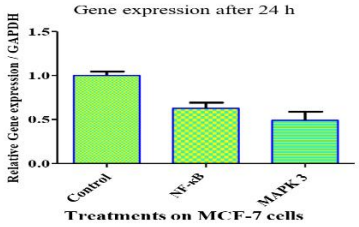

Figure 5. Expression of NF-κB and MAPK 3 on MCF-7 cells**.** Each value is the mean ± SEM (n=3), and One-way ANOVA (Dunnett post-test) analysis was performed.

GST, known as ligandins, comprise a family of eukaryote and prokaryotic phase II metabolic isozymes best known for their ability to catalyze the conjugation of the reduced form of GSH to a xenobiotic substrate for detoxification [34]. GSTs catalyze glutathione conjugation to a broad range of electrophilic, endogenous, and exogenous compounds. Glutathione conjugation is the first step in the mercapturic acid pathway that eliminates toxic compounds. The upregulation of GST suggests that it is involved in the MAPK pathway. According to Townsend [35], in controlling the MAP kinase pathway through protein-protein interactions, GST plays the main role. Specifically, GST has been shown to be a c-Jun N-terminal kinase 1 (JNK1) endogenous inhibitor, a kinase involved in stress response, apoptosis, and cell proliferation [22]. Isothiocyanates are a group of xenobiotics undergoing reversible GST-catalysed conjugation with GSH to form thiocarbamates to maintain cell homeostasis [35].

3.4. Morphology of MCF-7 cells after treatment with DMSO and BITC.

In this study, the further exploration of the morphological changes of MCF-7 cells after the treatment was investigated. The treated cells with 0.05% DMSO (vehicle control) and BITC showed an intact nuclear structure, as those treatments were not toxic toward MCF-7 cells. Meanwhile, late apoptotic cells can be seen on BITC-treated cells by the orange stain at the nuclear region since ethidium bromide incorporated the stain (Figure 6). Besides that, the blabbing and disruption of the membrane can be seen as BITC-induced apoptosis in MCF-7 cells compared to the control. This was supported by Yi-Ping *et al*. [36], that BITC induced apoptosis in human cancer cells.

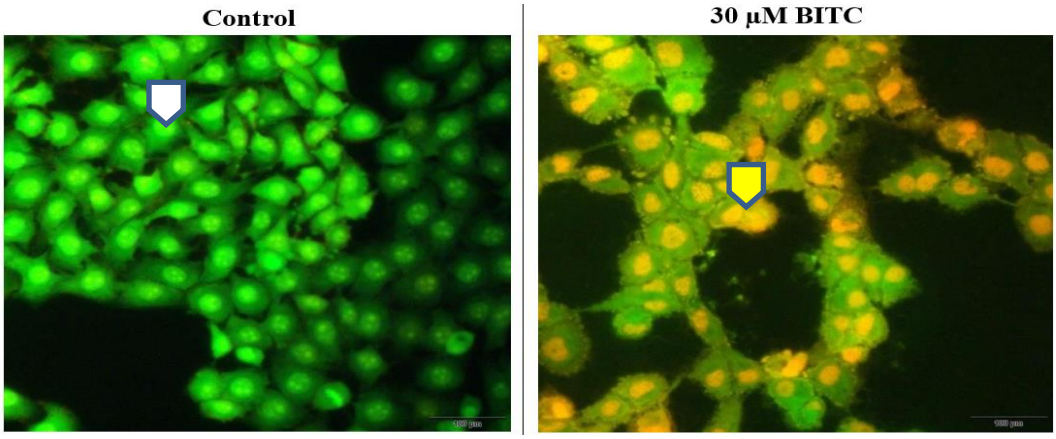

Figure 6. Morphology of MCF-7 cells after being treated with BITC (30 µM) at 24h after staining with AO/EB. The stained MCF-7 cells were characterized by viable–light green (shown by white arrows); early apoptotic–bright green with condensed chromatin or bright yellow nuclei, late apoptotic–orange nuclei (all apoptotic cells are shown by yellow arrow); were examined under a fluorescent microscope (X 400 magnification).

3.5. Caspase 3/7 level analysis of treated MCF-7 cells with BITC.

The disruption of the mitochondrial membrane leads to cytochrome c release and caspase 9 activations, followed by the activation of the caspase-3, -6, and -7 (Figure 7). Thus, we are measuring apoptosis by treatments using FLICA fluorescence dye that quantifies caspase 3/7 level. H_2O_2 was chosen as a positive control. Compared to all treatments, only BITC showed a significantly increased caspase 3/7 level at 6 h of exposure, which might explain the potent toxicity of BITC towards MCF-7 cells. Interestingly, the caspase 3/7 level significantly increased at 24 h of BITC treatment (excluding the positive control), indicating

that the apoptotic event of treated MCF-7 cells with BITC was due to the activation of caspase 3/7. This evidence has been supported by Chiu-Fang *et al*. [25] that BITC regulated caspase 3 and instigated the apoptotic events.

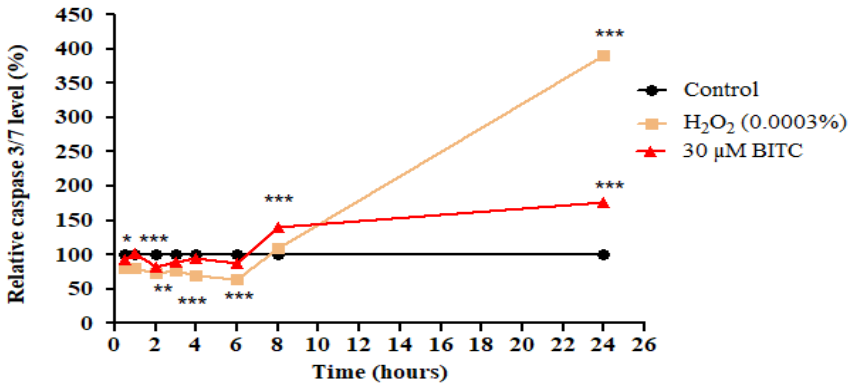

Figure 7. Caspase 3/7 level of treated MCF-7 cells with BITC (30 µM) at 30 min, 1h, 2h, 3h, 4h, 6h, 8h, and 24h as assessed by FLICA dye fluorometrically at excitation of 488 nm and emission of 530 nm. Each value is the mean ± SEM (n=3). Two-way ANOVA (Bonferroni post-test) analysis was performed. *P<0.05, **P<0.01, ***P<0.001 are significant differences compared to control.

3.6. Molecular docking analysis.

In the current study, BITC was found to have inhibitory properties against the development of human MCF-7 breast cancer by inhibiting the target enzyme participating in the growth and proliferation of cells. Therefore, the docking of BITC has been performed on two receptors named MTHFS (PDB:3HY3) and (EGFRK) domain (PDB:1M17) to understand the non-bonding interactions with amino acids forming the active sites of the receptors. The best pose of docked BITC with MTHFS with lower negative binding energy values that would have the maximum binding affinity with the receptor was chosen to visualize and analyze the results using Discovery studio (Figures 8a, 8b, and 8c).

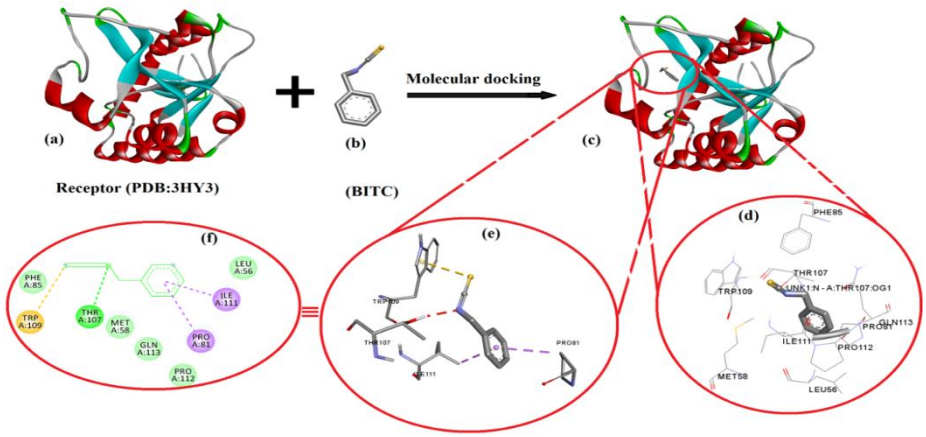

Figure 8. Binding mode of BITC with the receptor (PDB:3HY3); molecular docking interaction of **(a)** receptor, **(b)** BITC, **(c)** best-docked pose showing the active site where the compounds interact, **(d)** binding pose of the compound to the receptor showing various interactions and **(e)** ligand interaction to amino acids of receptor displaying with pi-interaction including hydrogen bond and **(f)** 2D diagram of receptor interactions to BITC.

The binding mode of the receptor compound showed a docking score of -5.40 kcal/mol and formed a hydrogen bond with amino acid THR107 to the nitrogen atom of the compound. Other amino acids formed the active sites of the receptor involved in the formation of a cavity around the compound using hydrophobic amino acids such as PRO81, ILE111, and

amphipathic TRP109 that were attached to BITC by sulfur atoms of the receptor with pi interactions of the aromatic ring of the compound including PRO112, GLN113, PRO81, PHE85, MET58, and LEU56 supported by close interactions with proper orientation of BITC in the cavity of the receptor (Figure 8e and 8f).

Another receptor, EGFR (epidermal growth factor receptor), played an essential role in the initiation and progression of breast cancer and was also used to perform a docking study to understand the interactions with the BITC ligand (Figure 9). The amino acid residues include LEU694, ALA719, LYS721, GLU738, LEU764, THR766, GLN767, LEU768, MET769, PRO770, PHE771, GLY772, LEU820, THR830, and ASP831 involved in the ligand binding pocket are confirmed based on non-binding interactions reported elsewhere [37]. The best pose of the docked compound with protein (PDB:1M17) was selected to know the interaction profiles and has a binding score of -4.88 kcal/mol and interacted with two hydrogen bonds with active amino acids GLN767 and MET769 as represented in figure (Figure 9a, 9b, 9c and 9d). Apart from hydrogen bonds, the docked pose (Figure 9e) revealed that hydrophobic interactions are a major force that bounds the ligand (BITC) in the binding pocket of hydrophobic amino acids such as LEU694, MET769, PRO770, and LEU768 using Pi-sigma, amide-pi stacked, and pi-alky interactions. Other hydrophobic residues in the binding cavity, such as ALA719, GLY772, LEU820, and GLN767, and polar residues like GLN767, and THR766, also play a role in protein-inhibitor interactions (Figure 9f). The combined modes of various binding interactions of the compound with MTHFS and EGFRK provide a stabilization system to protein-ligand complexes suppressing the uncontrolled growth and proliferation of MCF-7 breast cancer as expected by studying the nature and interaction of amino acids [37-39].

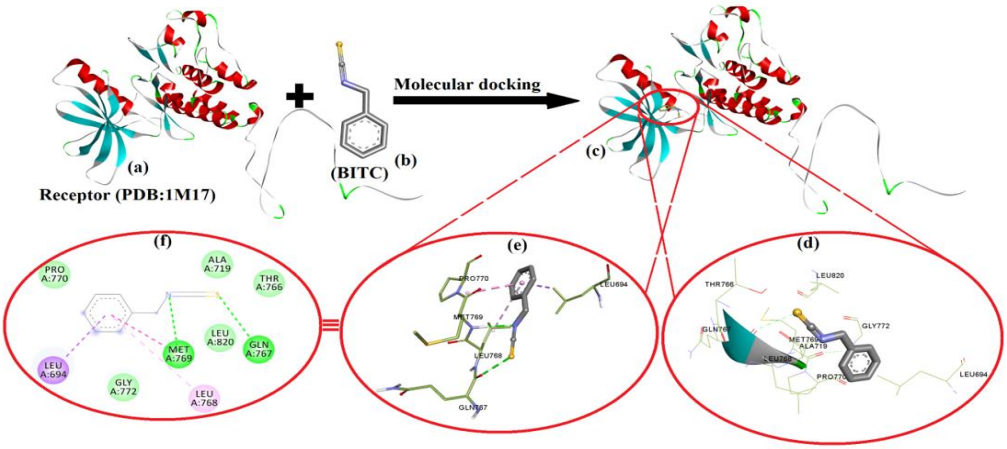

Figure 9. Binding mode for BITC with the receptor (PDB:1M17); molecular docking interaction of **(a)** receptor, **(b)** BITC, **(c)** best-docked pose showing the active site where the compounds interact, **(d)** binding pose of the compound to the receptor showing various interactions and **(e)** ligand interaction to amino acids of receptor displaying with pi-interaction including hydrogen bond and **(f)** 2D diagram of receptor interactions to BITC.

When BITC acts as a ligand and binds to EGFR, it triggers stress signaling, ROS, and oxidative stress conditions to induce MCF-7 cell death. According to this, the oxidative stress environment activated the MAPK pathway by upregulating p38 and downregulating ERK1/2 and pERK, which suppressed the growth of MCF-7 cells. At the same time, BITC activates antioxidant-responsive elements (AREs) by translocating NRF-2 (as the AREs transcription factor) into the nucleus. By activating ARE, the expression of GST is intensely upregulated to catalyze the conjugation between GSH and BITC. This GSH-BITC conjugation caused depletion of free GSH and thus resulting in the imbalance of redox homeostasis that will lead

to MCF-7 cell death (Figure 10). On the other hand, BITC can also bind with MTHFS receptor protein and potentially suppress DNA synthesis because BITC is able to become an inhibitor for MTHFS responsible for the conversion of 5-formyltetrahydrofolate to 5,10-methenyltetrahydrofolate [36].

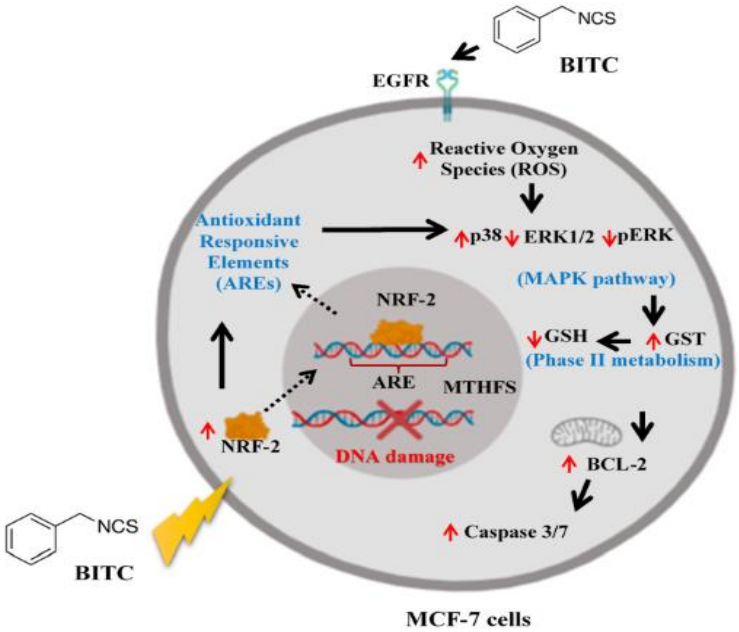

Figure 10. Schematic diagram on how BITC induced MCF-7 cell death. This diagram was generated using ©BioRender - https://biorender.com.

3.7. Quantification of BITC from Miswak extract.

Despite BITC acting as a cytotoxic agent that can inhibit MCF-7 cells, GC-MS plant extract analysis was conducted to evaluate the potential of some edible plants as chemopreventative agents.

From GC-MS analysis of Miswak water and methanol solvent extract, 4 and 37 compounds were identified (Figure 11), respectively. In the water extract, a negligible amount of BITC was found. However, in the methanol extract, BITC was the main abundant compound which was obtained at the retention time of 18.01 minutes. According to this study, the Miswak solvent extract contains 31.60% BITC. The other major compounds were n- Hexadecanoic acid (11.63%); cis-Vaccenic acid (9.62%); 9,12-Octadecadienoic acid (Z, Z) (6.78%), and Benzenemethanamine, N-(phenyl methylene) (5.27%).

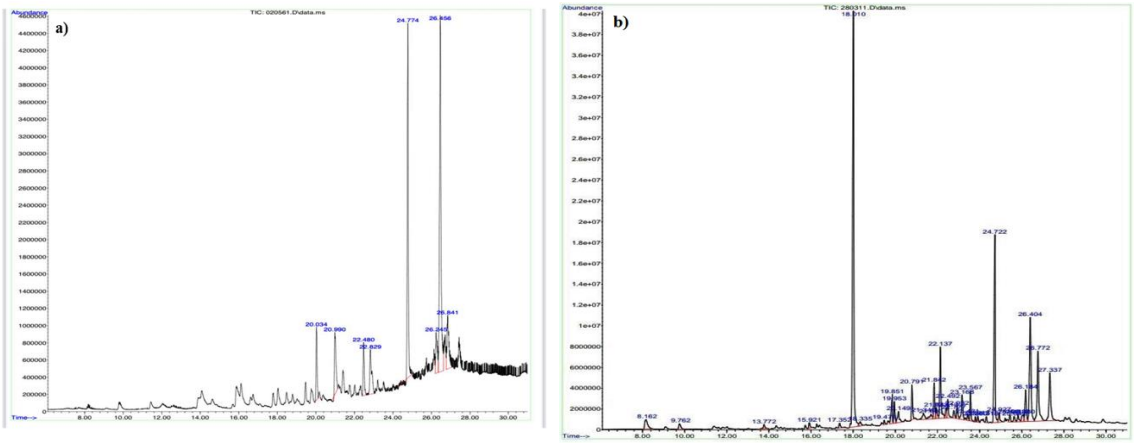

Figure 11. GC-MS fingerprint of **(a)** Miswak water extract and **(b)** Miswak methanol extract and standard BITC compounds with different concentrations.

The retention time for internal standards was recorded at 18.035, 18.08, 18.149, and 18.168 minutes, respectively, for different concentrations of standard BITC, and the retention times of BITC standards are almost the same as the retention time of BITC extracted from the Miswak (18.01 minute). The BITC peak in the methanol extract was found to be more prominent than the BITC peak in the water extract, indicating that methanol could be the best extraction solvent to extract BITC.

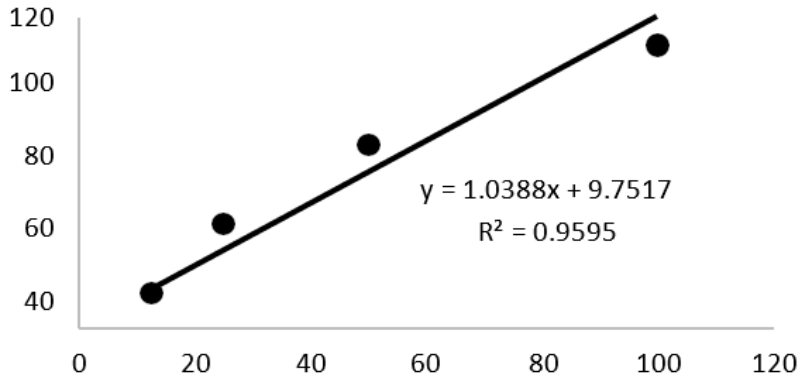

Figure 12. Standard curve for quantification of BITC.

The BITC was quantified with the calibration equation based on the peak area of internal BITC standards (Figure 12). The standard calibration equation was established using the abundance of peak area of a known amount (µg/ml) of standard pure compounds. The calibration equation for standard BITC is $y = 1.0388x + 9.7517$; $R^2 = 0.9595$. From the quantitative analysis by GC-MS/MS, the Miswak stick powder possesses 75.24 µg/20g Miswak powder. In spite of many studies have stated that water extraction could be the best method to activate myrosinase to yield isothiocyanates, epithionitriles, and nitriles in the hydrolysis process of glucosinolates, our water extraction result shows a negligible amount of BITC is obtained.

On the other hand, using the maceration extraction process with methanol-hexane, the yield percent of the extract is 6.25%. The previous study conducted by Abdel-Kader *et al*. [1] showed 0.073% (w/w) BITC from the ethanol extract of Miswak. In the current study, a very simple GC-MS method was used to quantify the BITC of the Miswak extract. Another research [40] showed that the ethanol extract of miswak contains 0.071 % of BITC, similar to BITC present in our Miswak extract. Therefore, it is important to determine the proper concentration of BITC in Miswak. So, it will be helpful to extract the pure BITC from Miswak commercially for real-life applications as a cost-effective natural extract with efficacy similar to or better than similar sources. Moreover, it will be beneficial to estimate the effectiveness of Miswak extract as a chemo-preventive agent.

4. Conclusions

In conclusion, the cytotoxicity effect of non-polar volatile properties of BITC that is present in a limited amount in the *Salvadora persica* (Miswak) extract on MCF-7 cancer cell lines as well as the normal human fibroblast cells was performed, and BITC was found toxic for cancer cell but not human fibroblast cell. Furthermore, the treated MCF-7 cell lines with BITC showed some changes in the regulation of NRF-2, p38, glutathione-S- transferase (GST), BCL-2, p-ERK, and ERK 1/2 protein expression, as well as NF-κB and MAPK gene expression, results in caspase 3/7 activation which leads to cell death. In addition, BITC was

molecular docked to two receptors, MTHFS and EGFRK, to establish interaction profiles with cavity-forming amino acids. THR107, PRO81, and ILE111 were among the active-side amino acids involved in hydrogen bond formation, with some forming pi interactions with the aromatic skeletons and functional groups of BITC. These interactions hold BITC in the active pockets of the receptor and are believed to inhibit the growth and proliferation of cancer cells. Therefore, further studies on the clinical trial of Miswak extract on cancer patients are needed. It possesses chemopreventative and therapeutic properties. Thus, the Miswak extract can be used as an effective chemo-preventive agent. Further investigation using *an in vivo* model to evaluate the efficacy of BITC in Miswak should be conducted in the future. The findings of such studies may offer hope in treating breast cancer.

Funding

This project was funded by the Ministry of Higher Education, Malaysia, and Universiti Malaysia Terengganu (UMT) under Grant Vot. 53131 and Universiti Kebangsaan Malaysia for the DIP-2018-007 grant.

Acknowledgments

The authors thank the Ministry of Higher Education, Malaysia, and Universiti Malaysia Terengganu (UMT). We also want to acknowledge the Central Laboratory of UMT, Faculty of Engineering and Built Environment, Universiti Kebangsaan Malaysia, and CRIM, UKM, for their support in conducting the research and analysis sample.

Conflict of Interest

The authors declare no conflict of interest.

References

1. Abdel-Kader, M.S.; Khamis, E.H.; Foudah, A.I; Alqarni, M.H. GC quantitative analysis of benzyl isothiocyanate in Salvadora persica roots extract and dental care herbal products. *Saudi Pharm J*. **2018** *26*, 462-466. https://doi.org/10.1016/j.jsps.2018.02.013
2. Jioe, I.P.J.; Lin, H.-L.; Shiesh, C.-C. The Investigation of Phenylalanine, Glucosinolate, Benzylisothiocyanate (BITC) and Cyanogenic Glucoside of Papaya Fruits (*Carica papaya* L. cv. 'Tainung No. 2') under Different Development Stages between Seasons and Their Correlation with Bitter Taste. *Horticulturae* **2022**, *8*, 198, 1-12. https://doi.org/10.3390/horticulturae8030198
3. Varadarajan, S; Madapusi, B.T.; Narasimhan, M.; Pandian,C.D.; Dhanapal, S. Anticancer Effects of Carica papaya L. and Benzyl Isothiocyanate on an Oral Squamous Cell Carcinoma Cell Line: An *In vitro* Study. *J. Contemp Dent Pract*. **2022**, *23*, 839–844. https://doi.org/10.5005/jp-journals-10024-3384
4. Rahaman, M. H.A.; Kadir, N.H.A.; Amin, N.M.; Omar, W.B.W. Cytotoxicity effect of water extracts of Moringa oleifera leaves and seeds against MCF-7 cells. *Acta Hortic*. **2017**, *1158*, 279-286. https://doi.org/10.17660/ActaHortic.2017.1158.31
5. Albabtain, R.; Azeem, M.; Wondimu, Z.; Lindberg, T.; Borg-Karlson, A.K.; Gustafsson, A. Investigations of a Possible Chemical Effect of Salvadora persica Chewing Sticks. *Evidence-based Complement Altern Med*. **2017**, 9-12. https://doi.org/10.1155/2017/2576548
6. EL-Hefny, M.; Ali, H.M.; Ashmawy, N.A.; Salem, M.Z.M. Chemical composition and bioactivity of salvadora persica extracts against some potato bacterial pathogens. *BioResources*. **2017**, *12*, 1835-1849. https://doi.org/10.15376/biores.12.1.1835-1849
7. Razis, A.F.A.; Mohd, N. Cruciferous vegetables: Dietary phytochemicals for cancer prevention. *Asian Pacific J Cancer Prev.* **2013**, *14*, 1565-1570. https://doi.org/10.7314/APJCP.2013.14.3.1565

8. Hsueh, C.W.; Chen, C.; Chiu, P.Y.; Chiang, N.N.; Lu, C.C.; Yang, J.S.; Chen, F.A. Anticancer effect of benzyl isothiocyanate on the apoptosis of human gemcitabine-resistant pancreatic cancer MIA PaCa-2/GemR cells (MIA RG100). *Phcog Mag* **2022**, *18*, 675-678.
9. Fahey, J.; Zalcmann, A. T.; Talalay, P. The chemical diversity and distribution of glucosinolates and isothiocyanates among plants. *Phytochemistry*. **2001**, *56*, 5-51. https://doi.org/10.1016/s0031-9422(00)00316-2
10. Dinh,T.N.; Parat, M-O.; Ong, Y.S.; Khaw, K.Y. Anticancer activities of dietary benzyl isothiocyanate: A comprehensive review. *Pharmacological Research* **2021**, *169*, 105666, 1-12. https://doi.org/10.1016/j.phrs.2021.105666
11. Kołodziejski, D.; Koss-Mikołajczyk, I.; Glatt, H.; Bartoszek,A. The comparison of cytotoxic and genotoxic activities of glucosinolates, isothiocyanates, and indoles. *Sci Rep* **2022** ,*12*, 1-13. https://doi.org/10.1038/s41598-022-08893-8
12. Henklewska, M.; Pawlak, A.; Li, R.F.; Yi, J.; Zbyryt, I.; Obmińska-Mrukowicz, B. Benzyl Isothiocyanate, a Vegetable-Derived Compound, Induces Apoptosis via ROS Accumulation and DNA Damage in Canine Lymphoma and Leukemia Cells. *Int J Mol Sci.* **2021**, *22*, 11772, 1-6. https://doi.org/10.3390/ijms222111772.
13. Li, H.; Ming, X.; Wang, Z.; Li, J.; Liang, Y.; Xu, D.; Liu, Z.; Hu, L.; Mo, H. Encapsulation of Benzyl Isothiocyanate with β-Cyclodextrin Using Ultrasonication: Preparation, Characterization, and Antibacterial Assay. *Foods* **2022**, *11*, 3724, 1-12. https://doi.org/10.3390/foods11223724
14. Po, W.W.; Choi, W.S.; Khing, T.M.; Lee, J.Y.; Lee, J.H.; Bang, J,S,; Min, Y.S.; Jeong, J.H.; Sohn, U.D. Benzyl Isothiocyanate-Induced Cytotoxicity via the Inhibition of Autophagy and Lysosomal Function in AGS Cells. *Biomol Ther* . **2022**, *1*, 30, 348-359. https://doi.org/10.4062/biomolther.2022.019
15. Nakamura, T.; Tsutsui, C.; Okuda, Y.; Abe-Kanoh, N.; Okazawa, S.; Munemasa, S.; Murata, Y.; Kato, Y.; Nakamura, Y. Benzyl isothiocyanate and its metabolites inhibit cell proliferation through protein modification in mouse preosteoclast RAW264.7 cells. *J. Biochem. Mol. Toxicol*. **2022**, *36*, e23184. https://doi.org/10.1002/jbt.23184
16. Park, W.S.; Lee, J.; Na, G.; Park, S.; Seo, S.K.; Choi, J.S.; Jung, W.K.; Choi, I.W. Benzyl Isothiocyanate Attenuates Inflammasome Activation in *Pseudomonas aeruginosa* LPS-Stimulated THP-1 Cells and Exerts Regulation through the MAPKs/NF-κB Pathway. *Int J Mol Sci.* **2022** , *23*, 1228, 1-10. https://doi.org/10.3390/ijms23031228
17. Hawraa, A.; Esraa, A.; Bhardwaj, G.R.; Areej, A. K.; Maribasappa, K. The Effect of Benzyl Isothiocyanate on the Expression of Genes Encoding NADH Oxidase and Fibronectin-Binding Protein in Oral Streptococcal Biofilms. *Frontiers in Oral Health* **2022**, *3*, 1-9. https://doi.org/10.3389/froh.2022.863723
18. Liu, J.; Zhang, K.; Wu, H.; Zhu, J.; Hao, H.; Bi, J.; Hou, H.; Zhang, G. Label-free quantitative proteomics reveals the antibacterial effects of benzyl isothiocyanate against Vibrio parahaemolyticus. *LWT* **2022**, *170*, 114050, 1-9. https://doi.org/10.1016/j.lwt.2022.114050
19. Li, H.; Ming, X.; Wang, Z.; Li, J.; Liang, Y.; Xu, D.; Liu, Z.; Hu, L.; Mo, H. Encapsulation of Benzyl Isothiocyanate with β-Cyclodextrin Using Ultrasonication: Preparation, Characterization, and Antibacterial Assay. *Foods*, **2022**, *11*, 3724, 1-12. https://doi.org/10.3390/foods11223724
20. Block, G.; Patterson, B.; Subar, A. Fruit, vegetables, and cancer prevention: A review of the epidemiological evidence. *Nutr Cancer*. **1992**, *18*, 1-29. https://doi.org/10.1080/01635589209514201
21. Sundaram, M.K.; Preetha, R.; Haque, S.; Akhter,N.; Khan, S.; Ahmad, S.; Hussain, A. Dietary isothiocyanates inhibit cancer progression by modulation of epigenome. *Seminars in Cancer Biology* **2022**. *83*, 353-376, https://doi.org/10.1016/j.semcancer.2020.12.021.
22. Davis, R.J. Signal transduction by the JNK group of MAP kinases. *Cell* **2000**, *103*, 239-252. https://doi.org/10.1016/S0092-8674(00)00116-1
23. Alam, M.B.; Ju, M.K.; Kwon, Y.G.; Lee, S.H. Protopine attenuates inflammation stimulated by carrageenan and LPS via the MAPK/NF-κB pathway. *Food Chem. Toxicol.* **2019**, *131*, 110583, 1-9. https://doi.org/10.1016/j.fct.2019.110583
24. Rahaman, M.H.A.; Kadir, N.H.A.; Omar, W.B.W. Synergism of benzyl isothiocyanate with quercetin, caffeic acid and caffeine to kill cancer cells: Who cares?. *Annals of Oncology* **2022**, *33*, S533. https://doi.org/10.1016/j.annonc.2022.05.312
25. Chiu-Fang, L.; Ni-Na, C.; Yao-Hua, L.; Yu-Syuan, H.; Jai-Sing, Y.; Shih-Chang, T.; Chi-Cheng, L.; Fu-An, C. Benzyl isothiocyanate (BITC) triggers mitochondria-mediated apoptotic machinery in human cisplatin-resistant oral cancer CAR cells. *Biomed*. **2018**, *8*, 13-22, https://pubmed.ncbi.nlm.nih.gov/30141402/.
26. Rao, C.V. Benzyl isothiocyanate: Double trouble for breast cancer cells. *Cancer Prev. Res*. **2013**, *6*. 760-763. https://doi.org/10.1158/1940-6207.CAPR-13-0242
27. Adler, V.; Yin, Z.; Tew, K.D.; Ronai, Z. Role of redox potential and reactive oxygen species in stress signaling. *Oncogene* **1999**, *18*, 6104-6111. https://doi.org/10.1038/sj.onc.1203128
28. Faraonio, R.; Vergara, P.; Paola, D.M.; Domenico, P.; Maria, G.P.; Maria, N.; Russo, T.; Cimino, F. p53 suppresses the Nrf2-dependent transcription of antioxidant response genes. *J Biol Chem*. **2006**, *281*, 39776-39784. https://doi.org/10.1074/jbc.M605707200

29. Finkel, T. Signal transduction by reactive oxygen species. *J. Cell Biol.* **2011**, *194*, 7-15. https://doi.org/10.1083/jcb.201102095
30. Ono, K.; Han, J. The p38 signal transduction pathway Activation and function. *Cell Signal*. **2000**, *12*, 1-13. https://doi.org/10.1016/S0898-6568(99)00071-6
31. Shen, T.; Miao, Y.; Ding, C.; Fan, W.; Liu, S.; Lv, Y.; Gao, X.; Boevre, M.D.; Yan, L.; Okoth, S.; Saeger, S.D.; Song, S. Activation of the p38/MAPK pathway regulates autophagy in response to the CYPOR-dependent oxidative stress induced by zearalenone in porcine intestinal epithelial cells. *Food Chem. Toxicol*. **2019**, *131*, 110527, 1-10. https://doi.org/10.1016/j.fct.2019.05.035
32. Sahu, R.P.; Batra,S.; Srivastava, S.K. Activation of ATM/Chk1 by curcumin causes cell cycle arrest and apoptosis in human pancreatic cancer cells. *Br. J. Cancer*. **2009**, *100*, 1425-1433. https://doi.org/10.1038/sj.bjc.6605039
33. Kasiappan,R.; Jutooru, I.; Karki, K.; Hedrick, E.; Safe, S. Benzyl isothiocyanate (BITC) induces reactive oxygen species-dependent repression of STAT3 protein by down-regulation of specificity proteins in pancreatic cancer. *J. Biol. Chem*. **2016**, *291*, 27122-27133. https://doi.org/10.1074/jbc.M116.746339
34. Zhang, Y.; Kolm, R.H.; Mannervik, B.; Talalay, P. Reversible conjugation of isothiocyanates with glutathione catalyzed by human glutathione transferases. *Biochem. Biophys. Res. Commun*. **1995**, *206*, 748-755. https://doi.org/10.1006/bbrc.1995.1106
35. Townsend, D.M; Tew, K.D. The role of glutathione-S-transferase in anticancer drug resistance. *Oncogene.* **2019**, *22*, 7369-7375. https://doi.org/10.1038/sj.onc.1206940.
36. Yi-Ping, H.; Yi-Wen, J.; Hsin-Yu, C.; Yung-Ting, H.; Shu-Fen, P.; Yu-Cheng, C.; Jiun-Long, Y.; Te-Chun,H.; Jing-Gung, C. Benzyl isothiocyanate induces apoptotic cell death through mitochondria-dependent pathway in gefitinib-resistant NCI-H460 human lung cancer cells *in vitro*. *Anticancer Res.* **2018**, *38*, 5165-5176. https://doi.org/10.21873/anticanres.12839
37. Wu, D.; Li, Y.; Song, G.; Cheng, C.; Zhang, R.; Joachimiak, A.; Shaw, N.; Zhi-Jie, L. Structural basis for the inhibition of human 5,10-methenyltetrahydrofolate synthetase by N10-substituted folate analogues. *Cancer Res.* **2009**, *69*, 7294-7301. https://doi.org/10.1158/0008-5472.CAN-09-1927
38. Sigismund, S.; Avanzato, D.; Lanzetti, L. Emerging functions of the EGFR in cancer. *Mol. Oncol.* **2018**, *12*, 3-20. https://doi.org/10.1002/1878-0261.12155
39. Stamos, J.; Sliwkowski, M.X.; Eigenbrot, C. Structure of the epidermal growth factor receptor kinase domain alone and in complex with a 4-anilinoquinazoline inhibitor. *J. Biol. Chem*. **2002**, *277*, 46265-46272. https://doi.org/10.1074/jbc.M207135200
40. Abdel-Kader, M.S.; Kamal, Y.T.; Alam, P.; Alqarni, M.H.; Foudah, A.I. Quantitative Analysis of Benzyl Isothiocyanate in *Salvadora persica* Extract and Dental Care Herbal Formulations Using Reversed Phase C18 High-Performance Liquid Chromatography Method. *Pharmacognosy Magazine* **2017**, *13*, S412-S416. https://doi.org/10.4103/pm.pm_117_17.